Thermo-Diffusion Effect on MHD Flow of Various Nano Fluids Past a Vertical Porous Plate

D. Dastagiri Babu*[1] , M. C. Raju[2] , S. Venkateswarlu[1] and E. Keshava Reddy[3]

[1] *Department of Mathematics, Rajeev Gandhi Memorial College of Engineering and Technology, Nandyal, Andhra Pradesh, India*
[2] *Department of Mathematics, JNTUA College of Engineering, Pulivendula, Andhra Pradesh, India*
[3] *Department of Mathematics, JNTUA College of Engineering, Anantapuramu, Andhra Pradesh, India*
***Corresponding author:** dastagiri478@gmail.com*

Abstract. An analytical model is employed for the nanofluid flow, heat and mass transfer from an infinite vertical plate in the presence of chemical reaction, and Soret effect. The governing equations that come from this are non-dimensionalized, transformed into a comparable form, and then solved using the three term perturbation technique and the accompanying boundary conditions. For this investigation, three different types of nano-fluids containing metallic nano particles as Cu (copper), and non-metallic nano particles as Al_2O_3 (alumina oxide), TiO_2 (titanium oxide) are considered, and water is considered as a base nanofluid. Using the MATLAB "Perturbation Method" and the findings already published in the literature, the resulting results are verified. It is described how important variables including the magnetic parameter, chemical reaction parameter, Soret number, the solid volume percentage of nanoparticles, the kind of nanofluid used, Nusselt number, Sherwood number and skin friction coefficient affect the flow. Tabular comparisons with published findings are shown.

Keywords. MHD, Soret effect, Cu water, Al_2O_3 water, TiO_2 water nano fluids

Mathematics Subject Classification (2020). 74H10, 35G20, 76W05

1. Introduction

Nanotechnology is now often employed in a variety of industrial applications. In order to make nanofluids, which have a far better thermal conductivity than normal fluids, nanometer-sized components are petrified in a conventional heat transmission fluid to boost heat transmission

capabilities. It was firstly developed by Choi and Eastmen [4]. According to research by Eastman *et al.* [7], a nanofluid containing water and 5% CuO nanoparticles may increase heat conductivity by up to 60%. In a circular tube with a fixed temperature, Heris *et al.* [10] inspected the laminar flow of convection heat transmission alumina oxide nanofluid. The convectional heat transmission and flow properties of a nanofluid based on Cu-H_2O were explored by Qiang and Yimin [22]. An investigational correlation for the thermal conductivity of Al_2O_3 water nanofluid as a function of nanoparticle size between 11mm and 150mm across a broad temperature range between 21 °C and 71°C was obtained by Chon *et al.* [5]. For enhanced heat transmission applications, Chopkar *et al.* [6] investigation looked at the production and characterisation of nanofluid. Sheikholeslami *et al.* [27] examined the nanofluid flow and heat transmission in a spinning device in the existence of a magnetic field. Albadr *et al.* [2] observed heat transmission along a heat transmission employing Al_2O_3 water nano fluid at various concentrations. The effect of the dispersion technique on the thermal conductivity and stability of nanofluids was covered by Nasiri *et al.* [19].

Santra *et al.* [25] investigated the heat transmission resulting from the laminal flow of copper water nano fluid across two parallel surfaces that had been isothermally heated. Mahdi *et al.* [16] investigated the impact of nano fluid on fluid flow and convective heat transmission in porous media. A numerical analysis of Cu water nano fluid in a square hollow with a conducting solid square cylinder at its centre was published by Sharma *et al.* [26]. Kuznetsov and Nield [15] studied the natural convective boundary layer flow of a nanofluid through a vertical plate. The numerical answer for a flow of mixed convection and edge layer in a nanofluid along a disposed plate submerged in a porous medium. The homotopy modeling of nanofluid dynamics from an isothermally growing, permeable sheet with transpiration was calculated by Rashidi *et al.* [24]. Rana *et al.* [23] looked into the numerical result for the drift of a nanofluid in a mixed convective boundary layer down an inclined plate embedded in porous material. In an annulus, Parvin *et al.* [20] evaluated the differential in thermal conductivity between the alumina water nano fluid and the surrounding water.

Owing to the strong influence of the magnetic field on the control of border layer flow and the enactment of numerous systems by means of electrically conducting field, such as MHD power generators, nuclear reactor cooling, plasma research, geothermal energy extraction, and so forth, there has been a resurgence in interest in MHD flow and heat transmission in permeable and clear domains. The heat transmission assorted convection slip flow through a vertical porous plate was examined by Mukhopadhyay and Iswar [18]. Kumar and Kumar [13] demonstrated the movement of a nanofluid over a vertical plate in an unstable MHD free convective boundary layer. Aly [3] observed the radiation and MHD boundary layer stagnation spots of the nanofluid flow toward a stretched sheet enclosed in the porous medium. Williamson nanofluid in porous media was studied by Konda *et al.* [12] for its impact on edge layer flow and melting heat transmission. A vertical plate imbedded in a permeable medium with a convective edge condition was used by Makinde and Aziz [17] to design the MHD mixed convection. The MHD oscillatory flow in a porous channel drenched with a permeable material was considered by Falade *et al.* [8]. Tripathy *et al.* [28] looked at the effect of a chemical reaction

on the MHD free convective surface over a moving vertical plate in a permeable medium. The erratic flow of multiple nano fluids via an accelerating vertical surface plate implanted inside a penetrable medium was premeditated by Hussanan *et al.* [11].

In light of the aforementioned findings, we investigate the heat transmission characteristics in flows of Cu and Al_2O_3, TiO_2 water-based nanofluids, as well as chemical reaction and the Soret effect. The three term perturbation approach is used to resolve the governing equations analytically. Prandtl number, suction parameter, magnetic field effects on the flow, velocity, temperature, and concentration disseminations are all provided together with the variables. The Soret number, the parameters include nusselt number, sherwood number and skin friction, nanoparticle volume segment. The findings are in strong accord with pertinent findings in the current literature.

2. Identification and Characterization of the Problem

Take a look at a two-dimensional steady edge layer of a nanofluid consisting of three various nano particles Cu, Al_2O_3, and TiO_2 water-based fluids flowing across an infinite plate in a uniformly free flow, as drawn in Figure 1. Assume that the nanofluid is in thermal evenness and that no-slip conditions occur among them. In the coordinate system, the x-axis runs parallel to the plate while the z-axis is perpendicular to it.
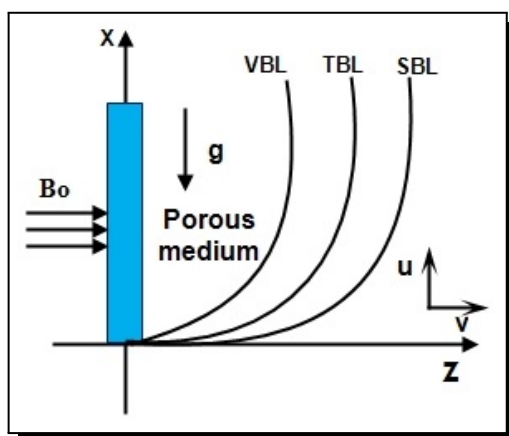
Figure 1. Physical model of the problem

Normal execution of the magnetic field strength (B_o) to the plate is made. In a stationary situation, the fluid is at the same heat and concentration as the plate, and when $t \geq 0$, the temperature T'_∞ and concentration C'_∞ at the platter vary harmonically with persistent mean.

A water-based nanofluid with three distinct kinds of nanoparticles —Cu, Al_2O_3, and TiO_2— makes up the fluid in the present challenge. It is envisaged that the nanoparticles would have a consistent size and shape. Additionally, it is anticipated that both fluid phase nanoparticles will be in a condition of thermal equilibrium. Table 1 lists the thermophysical characteristics of nanofluids. The governing equations are as follows after taking into account the prior hypotheses (Prasad *et al.* [21]):

$$\frac{\partial v'}{\partial z'} = 0, \tag{1}$$

$$\rho_{nf}\left[\frac{\partial u'}{\partial t'} + v'\frac{\partial u'}{\partial z'}\right] = \mu_{nf}\frac{\partial^2 u'}{\partial z'^2} + (\rho\beta)_{nf}g(T' - T'_\infty) + (\rho\beta^*)_{nf}g(C' - C'_\infty) - \frac{\mu_{nf}u'}{K'} - \sigma B_0^2 u', \tag{2}$$

$$\frac{\partial T'}{\partial t'} + v'\frac{\partial T'}{\partial z'} = \alpha_{nf}\frac{\partial^2 T'}{\partial z'^2} - \frac{Q'}{(\rho C_p)_{nf}}(T' - T'_\infty), \tag{3}$$

$$\frac{\partial C'}{\partial t'} + v'\frac{\partial C'}{\partial z'} = D_m\frac{\partial^2 C'}{\partial z'^2} - K_l(C' - C'_\infty) + \frac{D_m K_T}{T_m}\frac{\partial^2 T'}{\partial z'^2} \tag{4}$$

The initial and boundary conditions of the fluid flow are

$$\left.\begin{array}{ll} u'(z', t') = 0, \ T' = T'_\infty, \ C' = C'_\infty & \text{for } t' < 0 \\[4pt] u'(z', t') = U_0, \ T' = T'_w + [T'_w - T'_\infty]\varepsilon e^{iw't'} \\[4pt] C' = C'_w + [C'_w - C'_\infty]\varepsilon e^{iw't'} & \text{for } t' \geq 0 \text{ at } z' = 0 \\[4pt] u'(z', t') = 0, \ T' = T'_\infty, \ C' = C'_\infty & \text{at } z' \to \infty \end{array}\right\} \tag{5}$$

The equation (1) gives

$$v' = -V_0 \ (V_0 > 0). \tag{6}$$

Here V_0 is given as an unvarying suction velocity and it is pointed towards the plate with opposite sign.

For the nano fluids, the expression of density (ρ_{nf}), thermal diffusivity (α_{nf}), thickness of the nano fluid(μ_{nf}), thermal extension coefficient$[(\rho\beta)_{nf}]$, and capacity $[(\rho C_p)_{nf}]$ are defined as [28]

$$\rho_{nf} = (1 - \phi)\rho_f + \phi\rho_s, \quad \alpha_{nf} = \frac{K_{nf}}{(\rho C_p)_{nf}}, \quad \mu_{nf} = \frac{\mu_f}{(1 - \phi)^{2.5}},$$

$$(\rho\beta)_{nf} = (1 - \phi)(\rho\beta)_f + \phi(\rho\beta)_s, \quad (\rho C_p)_{nf} = (1 - \phi)(\rho C_p)_f + \phi(\rho C_p)_s$$

Nano fluids efficient thermal conductivity is deliberated by

$$\frac{K_{nf}}{K_f} = \left[\frac{K_s + 2K_f - 2\phi(K_f - K_s)}{K_s + 2K_f + 2\phi(K_f - K_s)}\right].$$

Introducing the following dimensionless variables,

$$u = \frac{u'}{U_0}, \quad z^* = \frac{U_0 z'}{v_f}, \quad t = \frac{U_0^2 t'}{v_f}, \quad w = \frac{w'v_f}{U_0^2}, \quad \theta = \frac{T' - T'_\infty}{T'_w - T'_\infty},$$

$$\psi = \frac{C' - C'_\infty}{C'_w - C'_\infty}, \quad Kr = \frac{K_1 v_f}{U_0^2}, \quad Pr = \frac{v_f}{\alpha_f}, \quad Gc = \frac{(\rho\beta^*)_{nf}g v_f(C'_w - C'_\infty)}{\rho_{nf}U_0^3},$$

$$Gr = \frac{(\rho\beta)_{nf}g v_f(T'_w - T'_\infty)}{\rho_{nf}U_0^3}, \quad K = \frac{K'\rho_f U_0^2}{v_f^2}, \quad S_c = \frac{v_f}{D_m}, \quad M = \frac{\sigma B_0^2 v_f}{\rho_{nf}U_0^2},$$

$$Q = \frac{Q'v_f^2}{K_f U_0^2}, \quad Sr = \frac{D_m K_T}{T_m}\frac{\partial^2\theta}{\partial z^2}\left[\frac{T'_w - T'_\infty}{C'_w - C'_\infty}\right]$$

Table 1. Physical characteristics of nanofluids and water [1]

Physical properties	ρ (kgm^{-3})	$\beta \times 10^{-5}$ (k^{-1})	k $(w\,m^{-1}k^{-1})$	C_p $(Jk^{-1}g^{-1}k^{-1})$
H$_2$O	997.1	21	0.613	4179
Cu	8933	1.67	400	385
Al$_2$O$_3$	3970	0.63	46	765
TiO$_2$	4250	1.05	8.90	686

The governing equations (2) to (4) are reduced to

$$A_1\left[\frac{\partial u}{\partial t} - s\frac{\partial u}{\partial z}\right] = A_4\frac{\partial^2 u}{\partial z^2} + A_2 G_r\theta + A_6 G_c\psi - \left[M + \frac{1}{K}\right]u, \tag{7}$$

$$A_3\left[\frac{\partial \theta}{\partial t} - s\frac{\partial \theta}{\partial z}\right] = \frac{1}{Pr}\left[A_5\frac{\partial^2 \theta}{\partial z^2} - Q\theta\right], \tag{8}$$

$$\frac{\partial \psi}{\partial t} - s\frac{\partial \psi}{\partial z} = \frac{1}{Sc}\frac{\partial^2 \psi}{\partial z^2} - Kr\psi + Sr\frac{\partial^2 \theta}{\partial z^2}. \tag{9}$$

The relative initial and boundary constraints in these non-dimensional form specifications are provided:

$$\left.\begin{array}{lll} u = 0, \ \theta = 0, \ \psi = 0 & \text{for } t < 0 \\ u = 1, \ \theta = 1 + \varepsilon e^{iwt}, \ \psi = 1 + \varepsilon e^{iwt} & \text{for } t \geq 0 \text{ at } z = 0 \\ u = 0, \ \theta = 0, \ \psi = 0 & \text{for } t \to \infty \end{array}\right\} \tag{10}$$

3. Solution of the Problem

The following three term perturbation approach is used to resolve the coupled nonlinear structure of equations (7) to (9) and the boundary conditions (10). Assumed are the following formulae for velocity, temperature, and concentration:

$$u = u_0(z) + \varepsilon e^{i\omega t}u_1(z) + \varepsilon^2 e^{2i\omega t}u_2(z) + O(\varepsilon^3), \tag{11}$$

$$\theta = \theta_0(z) + \varepsilon e^{i\omega t}\theta_1(z) + \varepsilon^2 e^{2i\omega t}\theta_2(z) + O(\varepsilon^3), \tag{12}$$

$$\psi = \psi_0(z) + \varepsilon e^{i\omega t}\psi_1(z) + \varepsilon^2 e^{2i\omega t}\psi_2(z) + O(\varepsilon^3). \tag{13}$$

The following equations are produced by replacing calculations (11) to (13) into equations (7) to (9) and comparing harmonic and non-harmonic terms while ignoring high order components.

$$A_4\frac{d^2 u_0}{dz^2} + A_1 S\frac{du_0}{dz} - \left(M + \frac{1}{K}\right)u_0 = -A_2 Gr\theta_0 - (A_6 Gcb_1 + A_6 Gcb_2)\psi_0, \tag{14}$$

$$A_4\frac{d^2 u_1}{dz^2} + A_1 S\frac{du_1}{dz} - \left(M + \frac{1}{K} + i\omega A_1\right)u_1 = -A_2 Gr\theta_1 - (A_6 Gcb_2 + A_6 Gcb_4)\psi_1, \tag{15}$$

$$A_4\frac{d^2 u_2}{dz^2} + A_1 S\frac{du_2}{dz} - \left(M + \frac{1}{K} + 2i\omega A_1\right)u_2 = -A_2 Gr\theta_2 - (A_6 Gcb_5 + A_6 Gcb_6)\psi_2, \tag{16}$$

$$A_5\frac{d^2 \theta_0}{dz^2} + A_3 PrS\frac{d\theta_0}{dz} - \left(M + \frac{1}{K}\right)\theta_0 - Q\theta_0 = 0, \tag{17}$$

$$A_5\frac{d^2 \theta_1}{dz^2} + A_3 PrS\frac{d\theta_1}{dz} - (i\omega A_3 Pr + Q)\theta_1 = 0, \tag{18}$$

$$A_5\frac{d^2\theta_2}{dz^2} + A_3 Pr S\frac{d\theta_2}{dz} - (2i\omega A_3 Pr + Q)\theta_2 = 0, \tag{19}$$

$$\frac{d^2\psi_0}{dz^2} + Sc S\frac{d\psi_0}{dz} - Kr Sc\,\psi_0 = -Sr Sc\,m_2^2\theta_0, \tag{20}$$

$$\frac{d^2\psi_1}{dz^2} + Sc S\frac{d\psi_1}{dz} - Sc(Kr + i\omega)\psi_1 = -Sr Sc\,m_4^2\theta_1, \tag{21}$$

$$\frac{d^2\psi_2}{dz^2} + Sc S\frac{d\psi_2}{dz} - Sc(Kr + 2i\omega)\psi_2 = -Sr Sc\,m_6^2\theta_2 \tag{22}$$

The boundary conditions (10) become

$$\left.\begin{array}{l} \theta_0 = 1,\ \theta_1 = 1,\ \psi_0 = 1,\ \psi_1 = 1,\ u_0 = 1,\ u_1 = 0 \quad \text{at } z = 0 \\ \theta_0 = 0,\ \theta_1 = 0,\ \psi_0 = 0,\ \psi_1 = 0,\ u_0 = 0,\ u_1 = 0 \quad \text{at } z \to \infty \end{array}\right\} \tag{23}$$

Now, by solving the above system of equations, one can have

$$u(z,t) = (a_3 e^{-m_8 z} + a_4 e^{-m_2 z} + a_5 e^{-m_{14} z}) + \varepsilon(a_8 e^{-m_{10} z} + a_9 e^{-m_4 z} + a_{10} e^{-m_{16} z})e^{i\omega t}$$
$$+ \varepsilon^2(a_{13} e^{-m_{12} z} + a_{14} e^{-m_6 z} + a_{15} e^{-m_{18} z})e^{2i\omega t}, \tag{24}$$

$$\theta(z,t) = e^{-m_2 z} + \varepsilon(e^{-m_4 z})e^{i\omega t} + \varepsilon^2(e^{-m_6 z})e^{2i\omega t}, \tag{25}$$

$$\psi(z,t) = (b_1 e^{-m_2 z} + b_2 e^{-m_8 z}) + \varepsilon(b_2 e^{-m_4 z} + b_4 e^{-m_{10} z})e^{i\omega t} + \varepsilon^2(b_5 e^{-m_6 z} + b_6 e^{-m_{12} z})e^{2i\omega t}. \tag{26}$$

The plate's skin friction coefficient $Z = 0$ is given by

$$\tau = \left(\frac{\partial u}{\partial t}\right)_{z=0} = (-m_8 a_3 - m_2 a_4 - m_{14} a_5) + \varepsilon(-m_{10} a_8 - m_4 a_9 - m_{16} a_{10})e^{i\omega t}$$
$$+ \varepsilon^2(-m_{12} a_{13} - m_6 a_{14} - m_{18} a_{15})e^{2i\omega t}. \tag{27}$$

The plate's Nusselt number $Z = 0$ is given by

$$Nu = \left(\frac{\partial\theta}{\partial t}\right)_{z=0} = -m_2 + \varepsilon(-m_4)e^{i\omega t} + \varepsilon^2(-m_6)e^{2i\omega t}. \tag{28}$$

The Sherwood number at the plate $Z = 0$ is given by

$$Sh = \left(\frac{\partial\psi}{\partial t}\right)_{z=0} = (-m_2 b_1 - m_8 b_2) + \varepsilon(-m_4 b_2 - m_{10} b_4)e^{i\omega t} + \varepsilon^2(-m_6 b_5 - m_{12} b_6)e^{2i\omega t}. \tag{29}$$

4. The Findings and Discussion

To get a physical understanding of the issue, analytical computations are made for various values of the components that govern the flow characteristics, and the results are visually shown. We have presented the computational results in Figures 2-14. The comparison results described by Kumar *et al.* [14] are shown in Table 5 for various values of M and ϕ by taking $Pr = 6.2$ and $Sr = 0$.

The effects of thermodiffusion (Sr) on the velocity and concentration profiles of the nanofluids Cu water, Al_2O_3 water, and TiO_2 water are shown in Figures 2 and 3. These nanofluids were used as a test subject. It can be shown that increasing Sr values improve the distributions of velocity and concentration. It occurs as a result of the production of excess mass fluxes brought on by temperature gradients for increasing Sr levels. Additionally, increasing Sr levels increases the thickness of the thermal boundary layer.
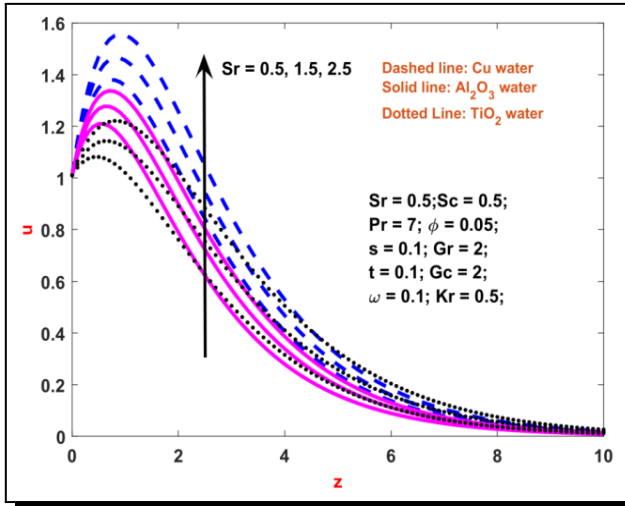
Figure 2. The velocity profile against *Sr*
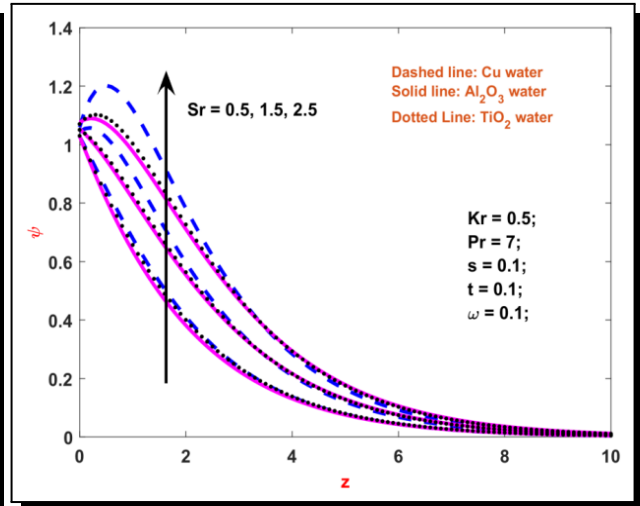
Figure 3. The concentration profile against *Sr*

The influence of nano particle volume fraction (φ) on concentration, heat, and velocity supplies are presented in Figures 4-6 for the nanofluids Cu water, Al_2O_3 water, and TiO_2 water, respectively. Figures 4 and 6 demonstrate that increasing the concentration and velocity distribution of the nanofluids made of Cu, Al_2O_3, and TiO_2 results in a drop in both, whereas Figure 5's temperature profile increases as the concentration of Cu, Al_2O_3, and TiO_2 increases. It happens as a outcome of the thermal edge layer, whose wideness decreases with cumulative values of. Figures 7-9 depict the velocity, temperature, and concentration circulations for different *Pr* values. When *Pr* values are raised, the velocity and heat profiles of nanofluids Cu water, Al_2O_3 water, and TiO_2 water become less noticeable. Low thermal diffusivity in big *Pr* fluids results in less heat transmission.
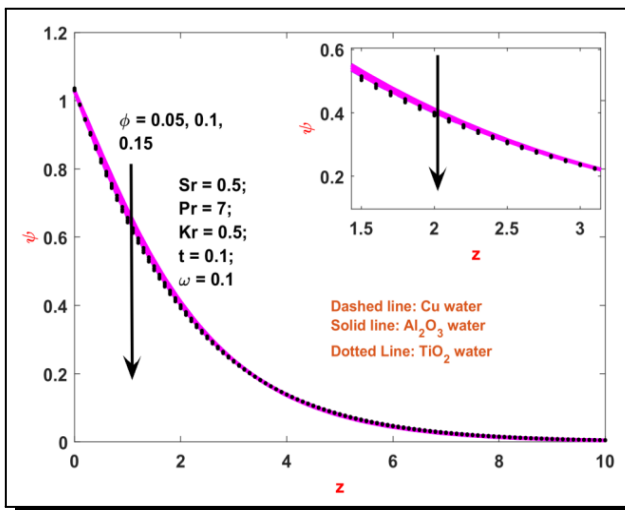
Figure 4. The concentration profiles against φ
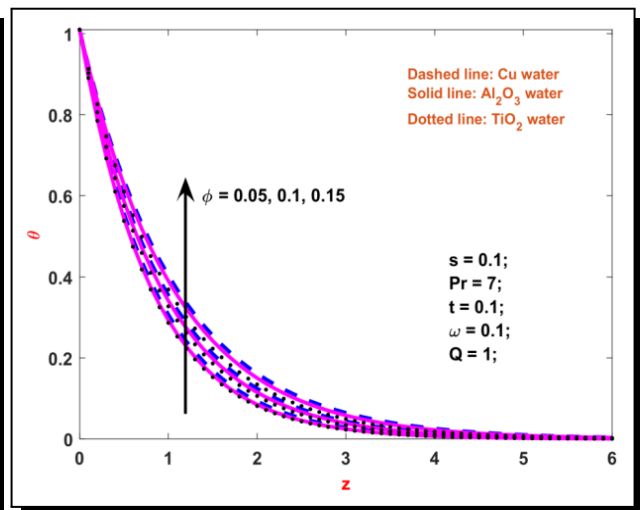
Figure 5. The temperature profiles against φ
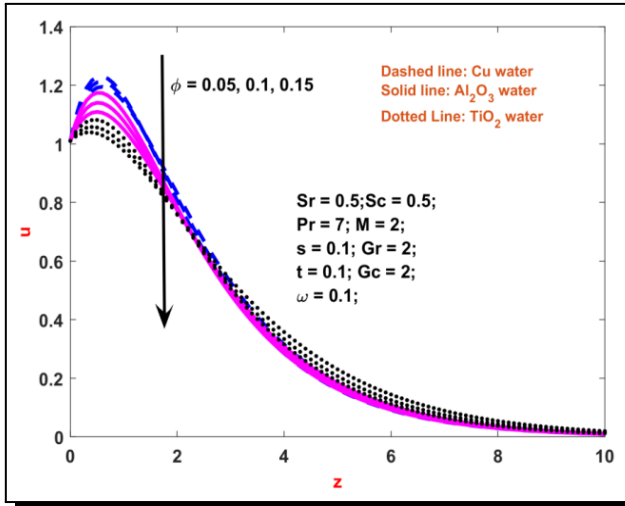
Figure 6. The velocity profiles against φ
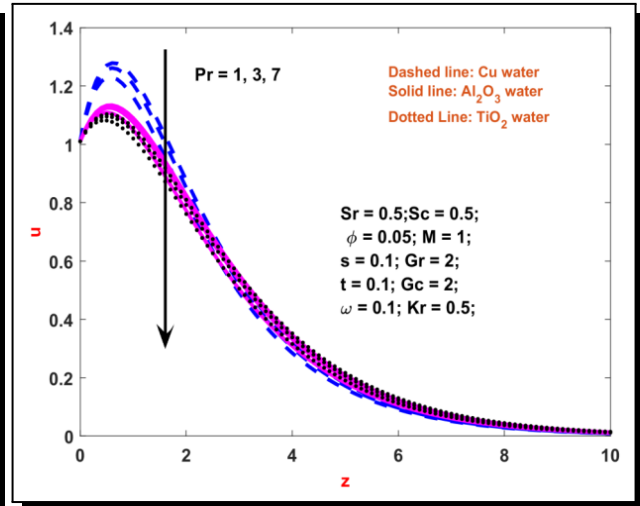
Figure 7. The velocity profiles against Pr
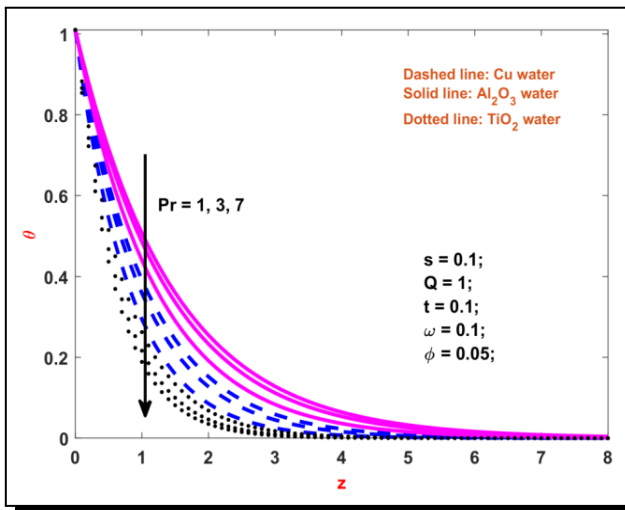
Figure 8. The heat results against Pr
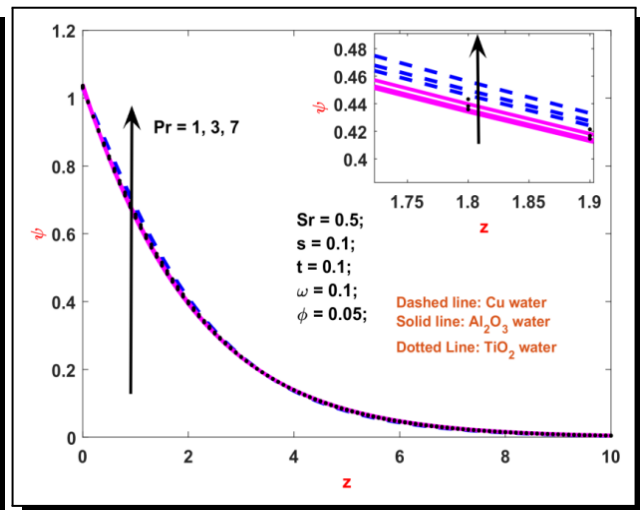
Figure 9. The concentration results against Pr
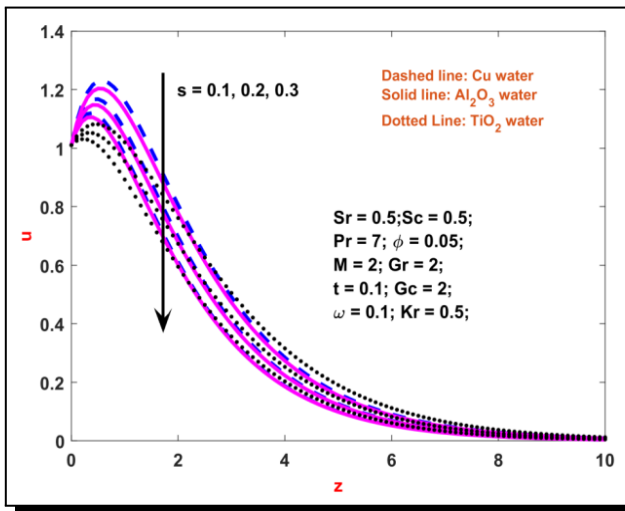
Figure 10. The velocity results against S
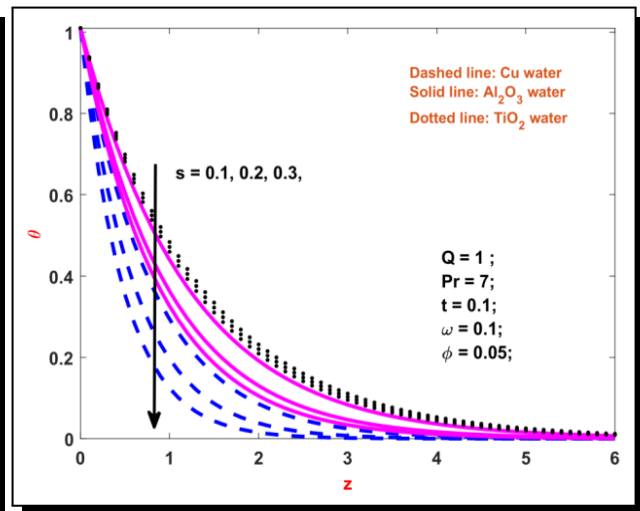
Figure 11. The temperature results against S
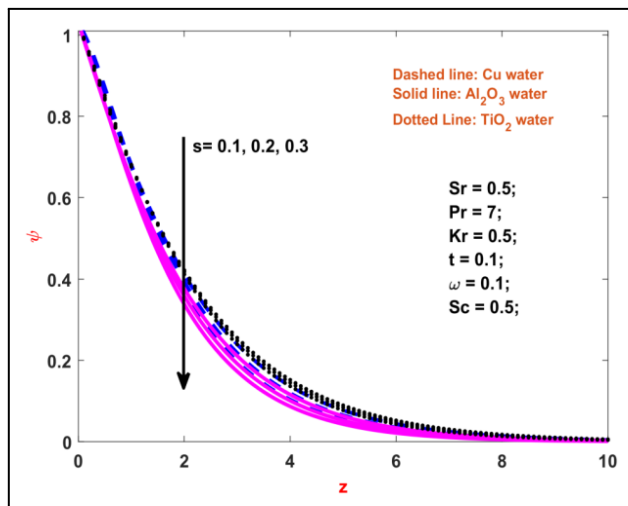
Figure 12. The concentration results against S
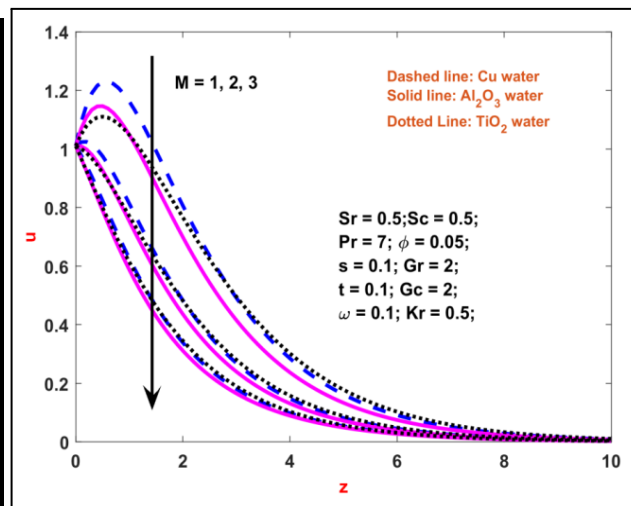
Figure 13. The velocity results against M
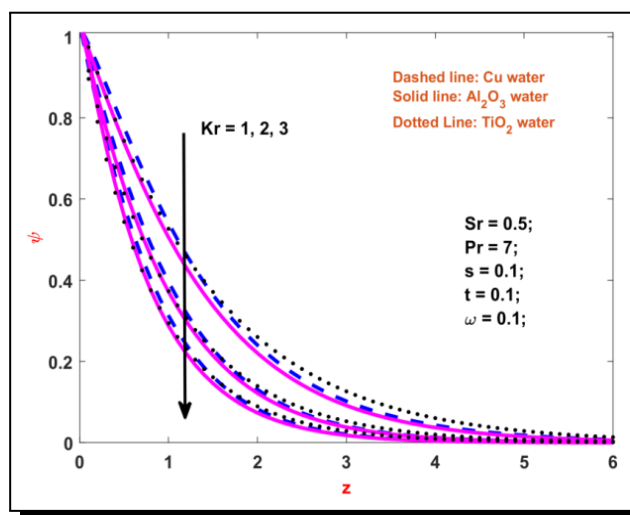
Figure 14. The concentration results against Kr

For nano fluids, the impacts of the suction (S) parameter are demonstrated in Figures 10–12, respectively, for velocity, temperature and concentration. It is observed that when suction (S) parameter values are increased, velocity, temperature, and concentration decrease. For both nano fluids Cu, Al_2O_3, and TiO_2, increasing the suction parameter (S) causes a decrease in the fluid's velocity across the boundary layer. S has a significant influence on fluid velocity in nano fluids containing the nanoparticles Cu, Al_2O_3, and TiO_2. Additionally, it is noted that Cu water has a greater maximum velocity than Al_2O_3 and TiO_2 do in the area. Figure 12 shows that S reduces the concentration profiles because, as is typical, the suction stabilizes border growth.

Figure 13 displays the velocity profiles decreases when enhancing the magnetic field (M) parameter for the nano fluids. These effects are very stronger near the surface of the plate. Applying a magnetic field to an electromagnetically controlled fluid provides a dragline energy that reduces flow velocity, which is consistent with this conclusion. Figure 14 predicts that

as the strength of chemical reaction (Kr) upsurges, the concentration profiles become slow down. It is due to the fact that various species concentration affects the rate of reaction of these mechanisms.

Increasing the Soret, Grashof, and modified Grashof numbers as well as the reversal behaviour seen in nano particle volume fraction limitation, magnetic limitation, and suction limitation for nano fluids Cu, Al$_2$O$_3$, and TiO$_2$, are all shown in Table 2 as increasing the skin friction values. Table 3 and Table 4 show the statistical values of the Nusselt number and Sherwood number for the nano particles Cu, Al$_2$O$_3$ and TiO$_2$, respectively. Table 3 provides the following information: it is perceived that the Sherwood number diminishes with enhancing the values of (S), (Q), while it enhances as increasing (φ). From Table 4, it is clear that Sherwood number raising as increase in the (Sr), (S) and it is diminishes as increase in the (Kr), and (φ) for the nano fluids Cu, Al$_2$O$_3$, and TiO$_2$.

Table 2. Skin friction coefficient (τ) by varying φ, M, S, Sr, Gr, Gc

φ	M	S	Sr	Gr	Gc	Cu-water	Al$_2$O$_3$-water	TiO$_2$-water
0.05	1	0.1	0.5	2	2	0.9266	0.8635	0.8582
0.10						0.8289	0.7122	0.7025
0.15						0.7348	0.5736	0.5600
	1.5					0.5239	0.4694	0.4649
	2					0.2075	0.1590	0.1550
	2.5					0.0562	0.0191	0.0137
		0.2				0.8034	0.7449	0.7387
		0.3				0.6833	0.6321	0.6253
		0.4				0.5675	0.5257	0.5186
			1			1.0634	0.9950	0.9915
			1.5			1.2002	1.1265	1.1247
			2			1.3370	1.2580	1.2545
				3		1.3206	1.2433	1.2344
				4		1.7147	1.6230	1.6107
				5		2.1087	2.0028	1.9869
					3	1.5574	1.4712	1.4672
					4	2.1182	2.0788	2.0761
					5	2.8190	2.6865	2.6851

Table 3. Nusselt number (Nu) by varying S, φ, Q

S	φ	Q	Cu-water	Al$_2$O$_3$-water	TiO$_2$ water
0.1	0.05	1	-1.2455	-1.2493	-1.2723
0.2			-1.6536	-1.6581	-1.6938
0.3			-2.1169	-2.1222	-2.1721
	0.10		-1.0899	-1.0969	-1.1379
	0.15		-0.9515	-0.9615	-1.0172
	0.20		-0.8259	-0.8387	-0.9072
		2	-1.6113	-1.6165	-1.6445
		3	-1.8961	-1.9022	-1.9343
		4	-2.1376	-2.1446	-2.1800

Table 4. Sherwood number (Sh) by varying S, Kr, Sr, φ

S	Kr	Sr	φ	Cu-water	Al$_2$O$_3$-water	TiO$_2$ water
0.1	0.5	0.5	0.05	-0.3441	-0.3431	-0.3371
0.2				-0.2644	-0.2632	-0.2536
0.3				-0.1680	-0.1665	-0.1528
	1.0			-0.6062	-0.6052	-0.5995
	1.5			-0.8060	-0.8050	-0.7991
	2.0			-0.9815	-0.9800	-0.9719
		0.6		-0.2935	-0.2923	-0.2851
		0.7		-0.2429	-0.2415	-0.2330
		0.8		-0.1923	-0.1907	-0.1809
			0.10	-0.3843	-0.3825	-0.3719
			0.15	-0.4195	-0.4170	-0.4028
			0.20	-0.4512	-0.4480	-0.4307

Table 5. Comparison of skin friction (φ) for $Pr = 6.2$, $Sr = 0$

M	Q	Cu-water	
		Sravan Kumar *et al.* [14]	Present study
0.5	0.5	0.63997	0.63896
1.0	1.0	0.57647	0.57266
2.0	2.0	0.56987	0.56757

5. Conclusions

In this work, heat source/sink, chemical reaction, and Soret effect are used to examine the temperature and mass transmission properties of Cu-water, Al_2O_3-water, and TiO_2 water based nano fluids across permeable media while using a magnetic field. A three-term perturbation approach is used to solve the governing equations. The findings are as follows:

(i) Al_2O_3-water and TiO_2-water based nano fluid displays thicker velocity boundary than Cu-water based nano fluid. The thickness of the momentum boundary layer decreases as the density of suction at the plate surface rises.

(ii) As enhancing the Soret (Sr) number, the velocity and concentration profiles are also increases in Cu, Al_2O_3, and TiO_2 nano fluids.

(iii) Al_2O_3-water and TiO_2-water based nano fluid displays thicker thermal boundary than Cu-water based nano fluid. The thermal boundary thickness diminishes when enhancing the suction (S) parameter and Prandtl (Pr) number whereas it enhances with rising numbers of nano particle volume segment (φ) parameter.

(iv) When the numbers of nano particle volume fraction (φ) parameter enhances, the velocity and concentration profiles are increases in Cu, Al_2O_3, and TiO_2 nano fluids.

(v) An enhance in Sr, Gr, and Gc increases the skin friction coefficient while the opposite behaviour is perceived with enhancing the φ, M and S.

(vi) Increases in S and Q parameters decrease the Nusselt number whereas the opposite behaviour is observed in φ.

(vii) The mass transmission rate at the plate surface rises as the Sr, S increases and decreases as the Kr, φ.

Nomenclature

u, v Velocity field components in x, z direction (ms^{-1})

Gc Mass Grashof value

Gr Thermal Grashof value

M Magnetic field

Pr Prandtl number

T Temperature (T)

S Suction/injection parameter

Sc Schmidt number

Sh Sherwood number

Sr Soret number

Nu Nusselt number

Q Heat source

Kr Chemical reaction parameter

Greek Symbols

α Thermal diffusivity

ρ Density of fluid (kg/m^3)

μ Dynamic viscosity (kgm^{-1}s^{-1})

φ Volume fraction of nano fluid (mg)

θ Dimensionless temperature

ν Kinematic viscosity (m^{2}s^{-1})

σ Electrical conductivity (sm^{-1})

β Thermal expansion coefficient (K^{-1})

Subscripts

f Fluid

s Nano particle

nf Nano fluid

Competing Interests

The authors declare that they have no competing interests.

Authors' Contributions

All the authors contributed significantly in writing this article. The authors read and approved the final manuscript.

References

[1] W. Abbas and M. M. Magdy, Heat and mass transfer analysis of nanofluid flow based on Cu, Al$_2$O$_3$ and TiO$_2$ over a moving rotating plate and impact of various nanoparticle shapes, *Mathematical Problems in Engineering* **2020** (2020), Article ID 9606382, 12 pages, DOI: 10.1155/2020/9606382.

[2] J. Albadr, S. Tayal and M. Alasadi, Heat transfer through heat exchanger using Al$_2$O$_3$ nanofluid at different concentrations, *Case Studies in Thermal Engineering* **1**(1) (2013), 38 – 44, DOI: 10.1016/j.csite.2013.08.004.

[3] E. H. Aly, Radiation and MHD boundary layer stagnation-point of nanofluid flow towards a stretching sheet embedded in a porous medium: analysis of suction/injection and heat generation/absorption with effect of the slip model, *Mathematical Problems in Engineering* **2015** (2015), Article ID 563547, 20 pages, DOI: 10.1155/2015/563547.

[4] S. U. S. Choi and J. A. Eastman, Enhancing thermal conductivity of fluids with nanoparticles, in: *Conference - 1995 International Mechanical Engineering Congress and Exhibition*, San Francisco, CA (United States), 12-17 November 1995, URL: https://www.osti.gov/biblio/196525.

[5] C. H. Chon, K. D. Kihm, S. P. Lee and S. U. S. Choi, Empirical correlation finding the role of temperature and particle size for nanofluid (Al$_2$O$_3$) thermal conductivity enhancement, *Applied Physics Letters* **87** (2005), 153107, DOI: 10.1063/1.2093936.

[6] M. Chopkar, P. K. Das and I. Manna, Synthesis and characterization of nanofluid for advanced heat transfer applications, *Scripta Materialia* **55**(6) (2006), 549 – 552, DOI: 10.1016/j.scriptamat.2006.05.030.

[7]   J. A. Eastman, U. S. Choi, S. Li, L. J. Thompson and S. Lee, Enhanced thermal conductivity through the development of nanofluids, in: *Nanophase and Nanocomposite Materials II*, S. Komarneni, J. C. Parker and H. J. Wollenberger (Eds.), Materials Research Society, Pittsburgh (1997), Symposium Proceedings, Vol. **457**, pp. 3 – 11, URL: https://apps.dtic.mil/sti/pdfs/ADA329567.pdf.

[8]   J. A. Falade, J. C. Ukaegbu, A. C. Egere and S. O. Adesanya, MHD oscillatory flow through a porous channel saturated with porous medium, *Alexandria Engineering Journal* **56**(1) (2017), 147 – 152, DOI: 10.1016/j.aej.2016.09.016.

[9]   M. A. A. Hamad, Analytical solution of natural convection flow of a nanofluid over a linearly stretching sheet in the presence of magnetic field, *International Communications in Heat and Mass Transfer* **38**(4) (2011), 487 – 492, DOI: 10.1016/j.icheatmasstransfer.2010.12.042.

[10] S. Z. Heris, M. N. Esfahany and S. Gh. Etemad, Experimental investigation of convective heat transfer of Al_2O_3/water nanofluid in circular tube, *International Journal of Heat and Fluid Flow* **28**(2) (2007), 203 – 210, DOI: 10.1016/j.ijheatfluidflow.2006.05.001.

[11] A. Hussanan, I. Khan, H. Hashim, M. K. Anuar, N. Ishak, N. M. Sarif and M. Z. Salleh, Unsteady MHD flow of some nanofluids past an accelerated vertical plate embedded in a porous medium, *Jurnal Teknologi* **78**(2) (2016), 121 – 126, DOI: 10.11113/jt.v78.4900.

[12] J. R. Konda, N. P. M. Reddy, R. Konijeti and A. Dasore, Effect of non-uniform heat source/sink on MHD boundary layer flow and melting heat transfer of Williamson nanofluid in porous medium, *Multidiscipline Modeling in Materials and Structures* **15**(2) (2019), 452 – 472, DOI: 10.1108/MMMS-01-2018-0011.

[13] T. S. Kumar and B. R. Kumar, Unsteady MHD free convective boundary layer flow of a nanofluid past a moving vertical plate, *IOP Conference Series: Materials Science and Engineering* **263**(6) (2017), 062015, DOI: 10.1088/1757-899X/263/6/062015.

[14] T. S. Kumar, P. A. Dinesh and O. D. Makinde, Impact of lorentz force and viscous dissipation on unsteady nanofluid convection flow over an exponentially moving vertical plate, *Mathematical Models and Computer Simulations* **12**(4) (2020), 631 – 646, DOI: 10.1134/S2070048220040110.

[15] A. V. Kuznetsov and D. A. Nield, Natural convective boundary-layer flow of a nanofluid past a vertical plate, *International Journal of Thermal Sciences* **49**(2) (2010), 243 – 247, DOI: 10.1016/j.ijthermalsci.2009.07.015.

[16] R. A. Mahdi, H. A. Mohammed, K. M. Munisamy and N. H. Saeid, Review of convection heat transfer and fluid flow in porous media with nanofluid, *Renewable and Sustainable Energy Reviews* **41** (2015), 715 – 734, DOI: 10.1016/j.rser.2014.08.040.

[17] O. D. Makinde and A. Aziz, MHD mixed convection from a vertical plate embedded in a porous medium with a convective boundary condition, *International Journal of Thermal Sciences* **49**(9) (2010), 1813 – 1820, DOI: 10.1016/j.ijthermalsci.2010.05.015.

[18] S. Mukhopadhyay and I. C. Mandal, Magnetohydrodynamic (MHD) mixed convection slip flow and heat transfer over a vertical porous plate, *Engineering Science and Technology, an International Journal* **18**(1) (2015), 98 – 105, DOI: 10.1016/j.jestch.2014.10.001.

[19] A. Nasiri, M. Shariaty-Niasar, A. Rashidi, A. Amrollahi and R. Khodafarin, Effect of dispersion method on thermal conductivity and stability of nanofluid, *Experimental Thermal and Fluid Science* **35**(4) (2011), 717 – 723, DOI: 10.1016/j.expthermflusci.2011.01.006.

[20] S. Parvin, R. Nasrin, M. A. Alim, N. F. Hossain and A. J. Chamkha, Thermal conductivity variation on natural convection flow of water–alumina nanofluid in an annulus, *International Journal of Heat and Mass Transfer* **55**(19-20) (2012), 5268 – 5274, DOI: 10.1016/j.ijheatmasstransfer.2012.05.035.

[21] P. D. Prasad, R. V. M. S. S. K. Kumar and S. V. K. Varma, Heat and mass transfer analysis for the MHD flow of nanofluid with radiation absorption, *Ain Shams Engineering Journal* **9**(4) (2018), 801 – 813, DOI: 10.1016/j.asej.2016.04.016.

[22] L. Qiang and X. Yimin, Convective heat transfer and flow characteristics of Cu-water nanofluid, *Science in China Series E: Technolgical Science* **45**(4) (2002), 408 – 416, DOI: 10.1360/02ye9047.

[23] P. Rana, R. Bhargava and O. A. Bég, Numerical solution for mixed convection boundary layer flow of a nanofluid along an inclined plate embedded in a porous medium, *Computers & Mathematics with Applications* **64**(9) (2012), 2816 – 2832, DOI: 10.1016/j.camwa.2012.04.014.

[24] M. M. Rashidi, N. Freidoonimehr, A. Hosseini, O. A. Bég and T.-K. Hung, Homotopy simulation of nanofluid dynamics from a non-linearly stretching isothermal permeable sheet with transpiration, *Meccanica* **49**(2) (2014), 469 – 482, DOI: 10.1007/s11012-013-9805-9.

[25] A. K. Santra, S. Sen and N. Chakraborty, Study of heat transfer due to laminar flow of copper–water nanofluid through two isothermally heated parallel plates, *International Journal of Thermal Sciences* **48**(2) (2009), 391 – 400, DOI: 10.1016/j.ijthermalsci.2008.10.004.

[26] B. Sharma, B. Kumar and R. N. Barman, Numerical investigation of cu-water nanofluid in a differentially heated square cavity with conducting solid square cylinder at center, *International Journal of Heat and Technology* **36**(2) (2018), 714 – 722, DOI: 10.18280/ijht.360238.

[27] M. Sheikholeslami, M. Hatami and D. D. Ganji, Nanofluid flow and heat transfer in a rotating system in the presence of a magnetic field, *Journal of Molecular Liquids* **190** (2014), 112 – 120, DOI: 10.1016/j.molliq.2013.11.002.

[28] R. S. Tripathy, G. C. Dash, S. R. Mishra and S. Baag, Chemical reaction effect on MHD free convective surface over a moving vertical plate through porous medium, *Alexandria Engineering Journal* **54**(3) (2015), 673 – 679, DOI: 10.1016/j.aej.2015.04.012.